Available online at www.sciencedirect.com
ScienceDirect
Planetary and Space Science 56 (2008) 1043–1053
Planetary and Space Science
www.elsevier.com/locate/pss

Accurate Mars Express orbits to improve the determination of the mass and ephemeris of the Martian moons

P. Rosenblatt[a,*], V. Lainey[b], S. Le Maistre[a], J.C. Marty[c], V. Dehant[a], M. Pätzold[d], T. Van Hoolst[a], B. Häusler[e]

[a]*Royal Observatory of Belgium (ROB), Av. Circulaire 3, B-1180 Uccle, Belgium*
[b]*IMCCE-Observatoire de Paris, UMR8028 du CNRS, 77 Av. Denfert-Rochereau, F-75014 Paris, France*
[c]*CNES/GRGS, 18 Avenue E. Belin, F-31401 Toulouse, Cedex 9, France*
[d]*Rheinisches Institut für Umweltforschung an der Universität zu Köln, Abt. Planetenforschung, Aachener Str. 209, 50931 Köln, Germany*
[e]*Institut für Raumfahrttechnik, Werner-Heisenberg-Weg 39, Universität der Bundeswehr München, D-85577 Neubiberg, Germany*

Received 21 November 2007; received in revised form 16 January 2008; accepted 5 February 2008
Available online 17 February 2008

Abstract

The determination of the ephemeris of the Martian moons has benefited from observations of their plane-of-sky positions derived from images taken by cameras onboard spacecraft orbiting Mars. Images obtained by the Super Resolution Camera (SRC) onboard Mars Express (MEX) have been used to derive moon positions relative to Mars on the basis of a fit of a complete dynamical model of their motion around Mars. Since, these positions are computed from the relative position of the spacecraft when the images are taken, those positions need to be known as accurately as possible. An accurate MEX orbit is obtained by fitting two years of tracking data of the Mars Express Radio Science (MaRS) experiment onboard MEX. The average accuracy of the orbits has been estimated to be around 20–25 m. From these orbits, we have re-derived the positions of Phobos and Deimos at the epoch of the SRC observations and compared them with the positions derived by using the MEX orbits provided by the ESOC navigation team. After fit of the orbital model of Phobos and Deimos, the gain in precision in the Phobos position is roughly 30 m, corresponding to the estimated gain of accuracy of the MEX orbits. A new solution of the *GM* of the Martian moons has also been obtained from the accurate MEX orbits, which is consistent with previous solutions and, for Phobos, is more precise than the solution from the Mars Global Surveyor (MGS) and Mars Odyssey (ODY) tracking data. It will be further improved with data from MEX-Phobos closer encounters (at a distance less than 300 km). This study also demonstrates the advantage of combining observations of the moon positions from a spacecraft and from the Earth to assess the real accuracy of the spacecraft orbit. In turn, the natural satellite ephemerides can be improved and participate to a better knowledge of the origin and evolution of the Martian moons.

PACS: 96.30.Gc; 96.30.Hf; 95.55.Pe; 95.10.Eg

Keywords: Mars; Martian satellites; Lunar planetary and deep-space probes; Orbit determination and improvement

1. Introduction

Since the space era, numerous efforts have been undertaken to develop accurate ephemerides of the Martian moons, Phobos and Deimos. On the one hand, accurate ephemerides are necessary for the spacecraft mission design and orbitography. On the other hand, the orbital motion of the Martian moons can be used to infer insight into the Martian interior. A key point in that respect is the tidal dissipation factor Q, which induces a secular acceleration on Phobos' orbital motion. As a consequence, such studies can provide some input for the study of the origin and evolution of the Martian moons.

For more than a century, several dynamical models of the orbital motion of these two moons have been developed and fitted to Earth-based observations and more recently to spacecraft observations (see Lainey et al., 2007 and

*Corresponding author. Tel.: +32 23736730; fax: +32 23749822.
E-mail address: Pascal.Rosenblatt@oma.be (P. Rosenblatt).

0032-0633/$ - see front matter © 2008 Elsevier Ltd. All rights reserved.
doi:10.1016/j.pss.2008.02.004

references therein). One of the latest observational sets was provided by cameras onboard spacecraft orbiting Mars like the Super Resolution Camera (SRC), part of the High-Resolution Stereo Camera (HRSC) onboard Mars Express (MEX) (Oberst et al., 2006). Recently, Lainey et al. (2007) have used SRC observations together with images from previous missions and Earth-based observations to derive a new ephemeris for the two moons. The post-fit residuals of this new ephemeris are less than a kilometer and reflect imperfections in the dynamical model that has been used, the error on the reduction of the astrometrical observations and the error on the spacecraft positions. For the SRC instrument, Lainey et al. (2007) have used the position of MEX provided by the flight dynamics team of the European Space Operation Center (ESOC). These MEX orbits have been designed for navigation purpose and may lack sufficient precision for the purpose of the precise determination of geophysical parameters such as the mass of the moons.

In this paper, the MEX orbits have been recomputed in order to improve both the accuracy of the MEX positioning and the precision of the derived Phobos and Deimos ephemerides. The radio-tracking data (Doppler and range) of MEX, acquired at Earth stations over the 2004–2006 period, have been used to fit a model of the MEX orbital motion. Section 2 describes the MEX dynamical model that has been used, Section 3 presents the results of the fit to tracking data, and Section 4 the improvement of the Phobos ephemeris when using the new accurate MEX orbits at the epoch of SRC observations. Section 5 shows a new estimation of the mass of the Martian moons obtained from the new accurate MEX orbits, and compares them with the most recent studies based on the radio-tracking data of the Mars Global Surveyor (MGS) and ODY spacecraft (Konopliv et al., 2006). The last section contains conclusions and perspectives.

2. MEX dynamical model and tracking data

The orbital period of MEX is roughly 6.7 h and the MEX altitude ranges from 250 km (pericenter pass) to 11 500 km (apocenter pass). Such an orbit is quite different from the usual near-circular orbits, such as those of the MGS and ODY spacecrafts, and therefore provides an opportunity to get additional information about geophysical parameters of Mars, such as the time variations of the gravity field due to seasonal mass transport in its atmosphere or tidal deformation induced by the Sun (Rosenblatt et al., 2005). In addition, the MEX orbit is expected to be more sensitive to the gravitational attraction of the Martian moons since its higher altitude allows closer Phobos encounter than MGS and ODY do. In order to have access to these effects through the monitoring of the MEX motion, we have determined an accurate orbit of MEX by using the Géodésie par Intégration Numérique Simultanée (GINS) software developed by the Centre National d'Etudes Spatiales (CNES) and further adapted at the Royal Observatory of Belgium (ROB) for planetary geodesy applications. In this software the equation of motion of the spacecraft is numerically integrated on the basis of a model of the forces acting on it. The partial derivatives of tracking observables with respect to several parameters of this model are simultaneously computed, allowing for an iterative least squares fit of the force model. All the gravitational and non-gravitational forces have been taken into account in the force budget. The latest spherical harmonic model of Mars' gravity field, JGM95J developed up to degree and order 95 and the associated Mars' rotation model (Konopliv et al., 2006) have been considered as well as a point mass representation of the Sun and other planets given by the JPL DE414 ephemeris (available at ftp://ssd.jpl.nasa.gov/pub/eph/planets/ascii/de414). To take into account the effect of the shortest wavelengths of Mars' gravity field on the MEX motion, we have chosen an integration time-step of 20 s. The gravitational attraction of the two Martian moons has also been modeled with a point mass representation, considering the latest estimates of their mass (Konopliv et al., 2006) and of their ephemeris (Lainey et al., 2007).

The non-gravitational forces act on each face of the spacecraft, which have been represented by flat plates (six for the bus and four for the two solar arrays) with known areas and optical properties. This representation of the spacecraft (called *macro-model*) needs to be oriented in space at any given time. The orientation of the bus with respect to an inertial frame has been modeled on the basis of sets of quaternion provided by ESOC. Since all the sets of quaternion for the orientation of the solar arrays with respect to the bus were not available, we have assumed that the solar arrays are oriented toward the Sun given the orientation of the bus (T. Morley, pers. comm., 2005). This assumption has been successfully tested over the February–July 2004 period, for which some sets of solar array quaternion were available (A. Konopliv, pers. comm., 2006). The *macro-model* and its orientation have allowed calculating the spacecraft acceleration due to the atmospheric drag (especially at altitude lower than 700 km) and the radiation pressure from both Sun and Mars (albedo and thermal infra-red emission). For the drag, we have used a model of the density of the Martian high atmosphere (DTM-Mars model, Bruinsma and Lemoine, 2002). The Mars radiation pressure has been modeled using spatially and temporally dependent models of the albedo and of the thermal emission (Lemoine, 1992). In addition to the drag and radiation pressure effects, a residual acceleration has been taken into account at each inertial wheel desaturation or Wheel off-Loading (WoL) event. Such events produce a change of velocity (or ΔV) of the spacecraft, which occurs once a day on average at the high altitude phase of the orbit. The spacecraft is then oriented in an attitude mode such that the ΔV is parallel to its velocity (Pulido-Cobo and Schoenmaekers, 2004). When projected into a frame tied to the spacecraft, the ΔV value is about one order of magnitude larger along the spacecraft

Z-axis than along both spacecraft X- and Y-axes. The three components of this residual or WoL acceleration have been calculated from the ΔV and duration of each event provided by ESOC. As the atmospheric density and the ΔV are not very well known, the associated forces are the most inaccurate ones of the force model. This inaccuracy is currently the main limit of the precise orbit determination of any spacecraft orbiting Mars (Rosenblatt et al., 2004; Konopliv et al., 2006), and thus of the determination of geophysical parameters from tracking data.

The tracking consists in measuring the round-trip time-delay (2-way range) and the 2-way Doppler shift of the carrier frequency (X-band at 8.5 GHz) of the radio link between the spacecraft and stations at the Earth's surface. The precision of the measurements is 1.2 mHz (or 0.02 mm/s in relative velocity) at 60-s integration time and 3 m for the Doppler and range, respectively. The tracking stations belong to the NASA Deep Space Network (DSN) located at Madrid (Spain) and Goldstone (California, USA) and to the ESA network (NNO station located at New Norcia, Australia). At a given time, the spacecraft is tracked by only one station, and the duration of each tracking pass varies from about 40 min to several hours. In one tracking pass, the Doppler signal is most often acquired every 60 s, while the ranging data are sparser (every 200 s on average). Since the tracking passes are not performed successively, gaps in the tracking coverage often occur, with a duration ranging from several hours to about 1 day. This non-continuous tracking limits the precision of the fit of the force model to the tracking data, especially at pericenter pass where the drag is maximal and at WoL events.

3. Fit of the MEX motion to the tracking data

The least squares fit to the Doppler and range tracking data has been performed on successive 7 calendar days data-arcs over the period from February 2004 to August 2006. We chose such duration of data-arc in order to compare the accuracy of our orbits with the accuracy of the ESOC orbits computed with similar data-arc duration. To initiate this iterative process we have taken the MEX position and velocity from the ESOC orbits for the initial state vector at the beginning of each data-arc. Since the WoL ΔV is not very well known, the residual acceleration must be adjusted at each event. As these events are not tracked from the Earth, we have added a priori constraints to the initial value of the residual acceleration. These constraints have been set as a fraction of the value of the largest component (along the Z-axis) of the residual acceleration, i.e. 10% of this value for the Z-axis component and 3% of this value for the X and Y components, respectively, as done by ESOC in their calculation of the navigation orbits (T. Morley, pers. comm., 2006). In addition to the three components of each WoL acceleration, we have fitted the initial state vector as well as scale factors for the drag and solar pressure radiation force. The fit of the scale factors is used to scale the associated force in order to compensate the inaccuracy of the force model, especially of the atmospheric density which is not very well known at an altitude of 250 km. We did not add any a priori constraints either on the scale factors or on the initial state vector. We have also fitted Doppler and range biases at each tracking pass in order to take into account systematic errors generated by the devices at each tracking station and an overall range bias for each data-arc to absorb systematic errors on the Mars–Earth position from the DE414 ephemeris.

In a procedure to get the geophysical signal from each data-arc, we have only selected the arcs for which the estimated value of the drag scale factor is between −10 and 10, for which the estimated value of the solar pressure factor is positive, and for which the rms of the Doppler post-fit residuals is smaller than 7.5 mHz. This selection represents 75% of all the data-arcs. The rms values of the post-fit residuals for these selected data-arcs are shown in Fig. 1. The average value has been found around 3.2 mHz (or 0.05 mm/s), which is in accordance with residuals found by Highsmith et al. (2004) for the February 2004 period. Some rms values are greater than 4 mHz, especially around September 2004, which corresponds to the solar conjunction period. The average of the rms values of the post-fit 2-way range residuals is less than 1 m, and represents the average precision of the MEX position relative to the Mars center-of-mass. These values of the Doppler and range residuals are similar to the ones obtained from fitting the MGS and ODY tracking data (Duron et al., 2006), thus meaning that the applied MEX dynamical model did not include large errors. The mean value of the estimated Doppler biases for each NNO and DSN station tracking pass is of the order of a few tenths of mHz, which is lower than the Doppler post-fit residuals for each data-arc. This implies that we have no large bias in the modeling of the Doppler shift measurements at each tracking station, including the new NNO ESA station. To estimate the error on the MEX positioning, we have performed orbit overlap differences between successive data-arcs (Fig. 2). The overlap duration has been chosen as 21 h or three revolutions of MEX around Mars. The larger differences are in the cross-track and along-track directions and vary from less than 1 to 100 m (sometimes up to 300 m, not shown in Fig. 2), with an average value of about 20–25 m. This is about 2 times lower than the average value of the ESOC orbit overlap differences (T. Morley, pers. comm., 2007). The overlap differences computed in this paper vary significantly between pairs of data-arcs. This is due to the tracking coverage, which varies from 20% to 80% of the data-arc duration (40% on average) between data-arcs. Indeed, the non-uniform tracking has a crucial consequence when the pericenter passes within a data-arc are not tracked (Fig. 3). In that case, the drag scale factor becomes negative, implying that the atmospheric density is negative, which is obviously impossible. In fact, due to correlations between the drag scale factor, the adjusted

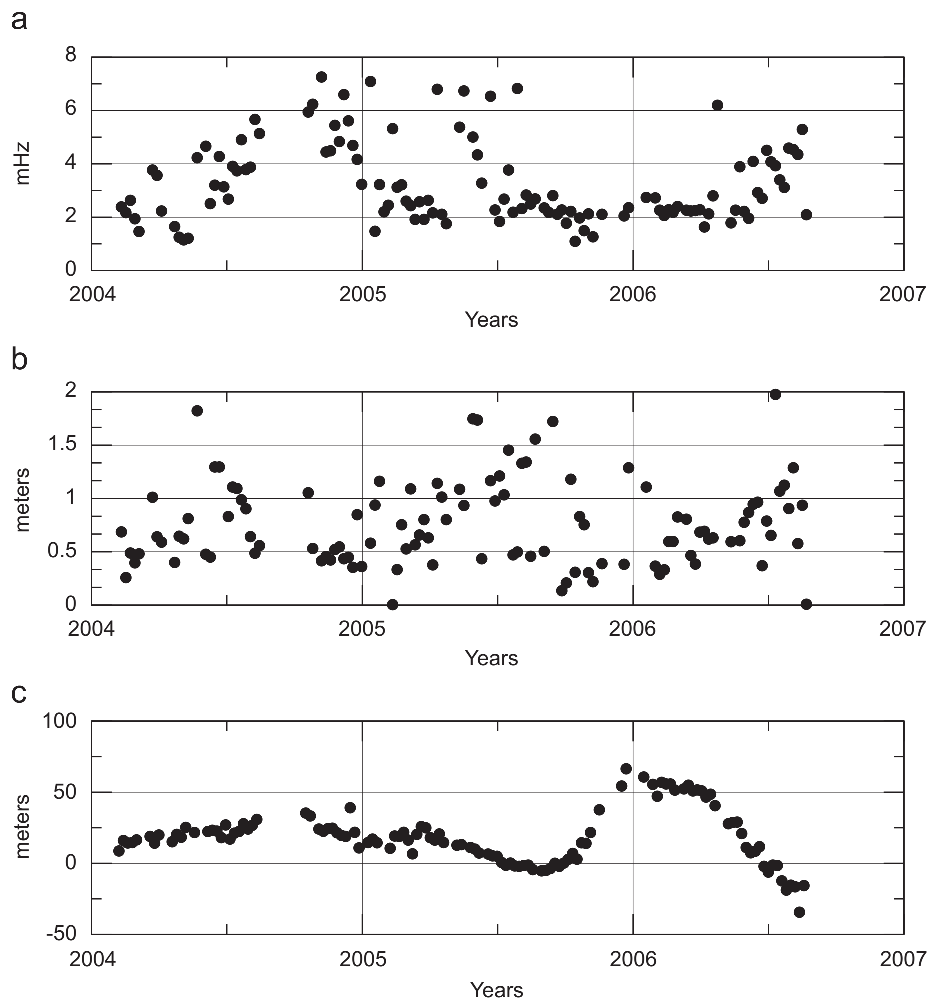

Fig. 1. RMS values of the post-fit residuals for each 7 days data-arc: (a) 2-way Doppler and (b) 2-way range. (c) Range bias corrections to the DE414 ephemeris estimated for each data-arc.

WoL accelerations and the initial state vector, the drag scale factor absorbs information from other phenomena. This situation especially occurs during about three successive months in the first half of 2006 (Fig. 3). When taking tight a priori constraints (about 0.04) for the drag scale factor, it was possible to estimate non-negative values for all the data-arcs even for those with a poor tracking coverage at pericenter passes. Nevertheless, the orbit overlap differences were not significantly improved. We have also tried to use the Stewart (1987) model instead of the DTM model for the density of Mars' high atmosphere. The values of the drag scale factor did not change, except for the second part of 2005, where the Stewart model has yielded lower scale factor values by a factor of about 2. However, the orbit overlap differences did not change, which confirms that the resolution of the drag acceleration is not limited by the a priori atmospheric model. The gaps in the tracking also occur systematically around the WoL events. As a consequence, the WoL residual acceleration cannot be perfectly adjusted and the corrections to the ESOC initial value are on average tens of percent and sometimes up to 600%, especially for the low amplitude X and Y components (Fig. 4). We have tried to take tighter a priori constraints for the WoL acceleration, but the orbit overlap differences were not significantly improved. The difficulty to properly adjust both drag effect and WoL acceleration effect has prevented to get the orbit overlap systematically below 10 m. The solar pressure scale factor shows a linear trend over the 2004–2006 period (Fig. 3). However, such trend is not observed in the orbit overlap differences (Fig. 2), thus it cannot come from errors in our orbit computation. This trend could come from variations of physical properties of the faces of the spacecraft such as temperature variations or the darkening of these faces with time. However, we did not get information to check such explanation.

The position of MEX relative to the Earth-based tracking stations is biased due to errors on the Mars position given by the DE414 ephemeris. The estimation of this bias per data-arc is displayed in Fig. 1. A quasi-constant value of about 20 m has been found up to April 2005. For the same period, the range bias from MGS and

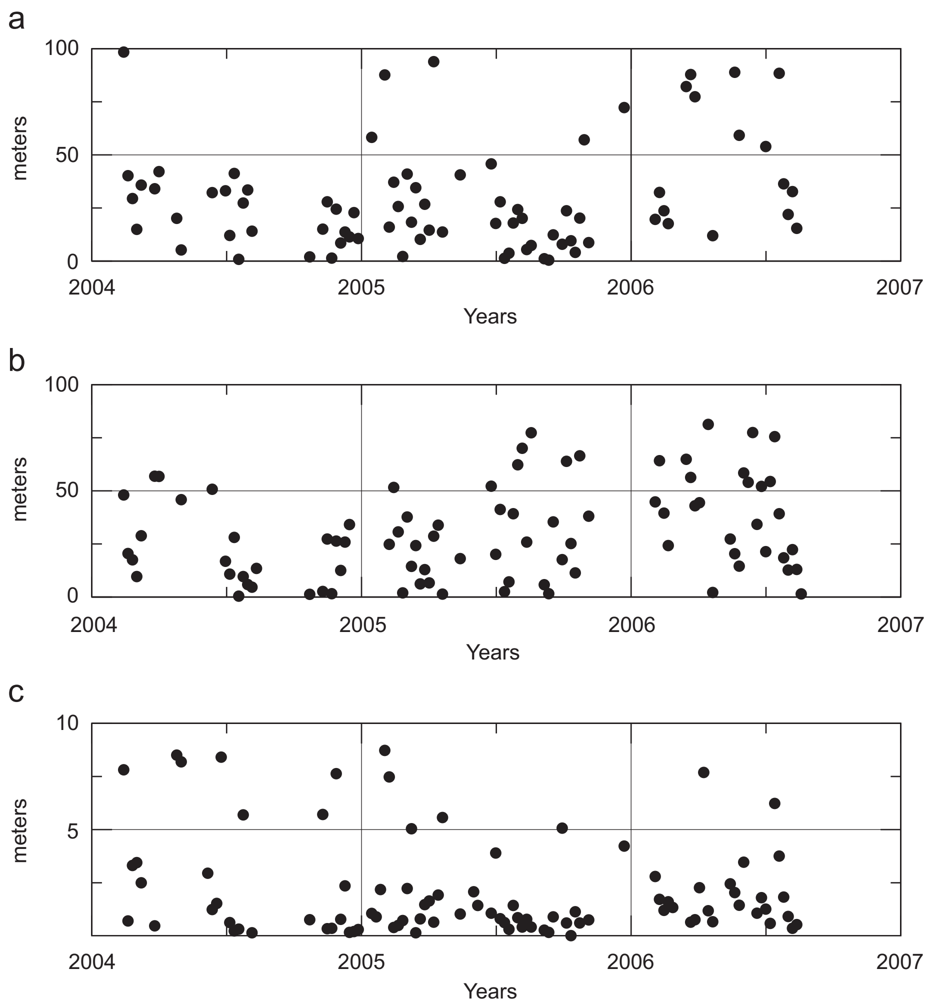

Fig. 2. RMS value of the overlap differences. They correspond to the rms of the MEX position differences between successive 7 days data-arcs over overlap duration of 21 h. (a) Along-track direction, (b) normal to the orbit plane, and (c) radial direction.

ODY data is about 1–2 m (Konopliv et al., 2006; Folkner, 2007). The MEX range bias value of 20 m probably reflects the residual errors in the MEX orbit related to the imperfect fit of the drag and WoL residual accelerations. An alternative explanation is that unmodeled additional time-delays have been generated by the transponder onboard MEX due to either temperature variations or electronic perturbations from other devices. On the other hand, it seems difficult to explain about 60 ns of time-delay from such perturbations (T. Morley, pers. comm., 2007). After 2005, the values of the estimated range bias vary with a peak-to-peak amplitude of about 50 m in addition to the previous 20 m value. Such a variation with the same amplitude is also observed on the range bias estimated from the MGS and ODY range tracking data for the same period (Folkner, 2007). This reflects residual errors in the DE414 ephemeris for which no range data from spacecraft have been introduced after April 2005.

To check if the choice of the 7 days duration for the data-arcs was optimal for the fit of the MEX dynamical model, we have tried shorter and longer data-arc duration (4, 8 and 10 days). We have obtained similar orbit overlap differences and values for the dynamical parameters, as for 7 days data-arc duration. We have also tried data-arcs that did not contain WoL events. The data-arc duration is then 1 day on average (2 days for the first months of 2004). In that case, a larger proportion of data-arcs have very little tracking data available at their pericenter passes, and the estimation of negative value for the drag scale factor occurs more frequently than for longer data-arcs. This seems to indicate that the drag acceleration is not better resolved over the 2004–2006 period with these shorter data-arcs than with longer data-arcs. We were not able to quantify the precision of the orbits from the shorter data-arcs since they are not overlapping.

4. Improvement of the Martian moon ephemerides

In principle the improvement of the accuracy of the MEX orbit should further improve the measured position, and after a new fit of these positions, the ephemeris of the Martian moons by the same order of magnitude (Fig. 5).

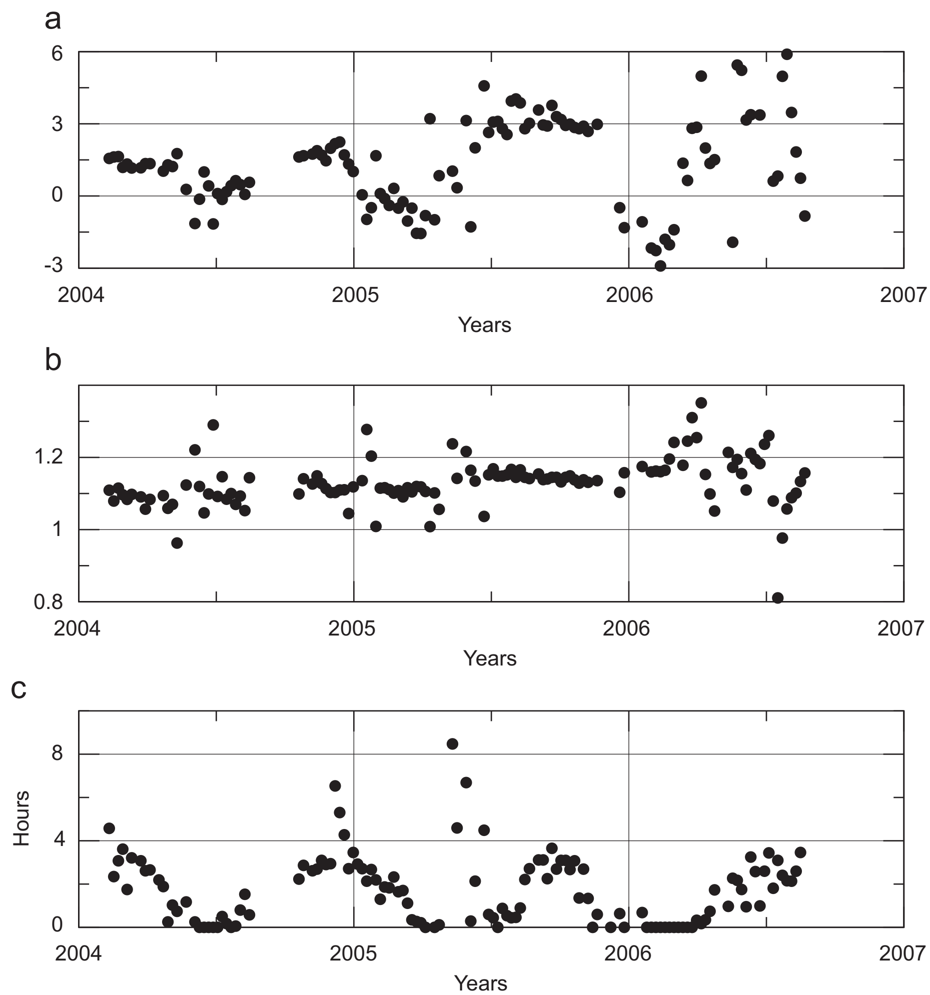

Fig. 3. Fit of the scale factor of the (a) atmospheric drag and (b) solar pressure accelerations for each 7 days data-arc. The drag factor represents the correction to the model of the atmospheric density used in the MEX dynamical model (see text). (c) Doppler tracking coverage at pericenter passes (altitude <700 km) for each data-arc (expressed in hours).

Lainey et al. (2007) showed that the accuracy of the SRC observations is roughly 3 km, which is still too large and will not benefit from the gain in accuracy of the MEX orbits computed in this paper. Recently, a new set of SRC observations have been reduced by Willner et al. (2007). The related accuracy reaches a few hundred of meters. Hence, the improvement of the moon ephemeris, which is expected when using the ROB MEX orbits, may be assessed. We used these new SRC observations to derive two new solutions for the Martian moon positions: one using the ROB MEX orbits (solution 1) and the other one using the ESOC MEX orbits (solution 2). We have used exactly the same method and software to derive these positions as in Lainey et al. (2007). Besides the MEX observations, all other spacecraft and Earth-based observations have also been considered. The same procedure for weighting the different observational sets has been used. It relies on an estimation of the sigma for each data set provided by a former iteration in the least squares fit. A 3-sigma criterion has been applied to reject poor observations. With the selected MEX data-arcs of the previous section, we have been able to use the more accurate ROB MEX orbits instead of the ESOC orbits for 34 SRC observations of Phobos.

Fig. 6 and Table 1 display a comparison of the post-fit residuals in right ascension and declination between Phobos positions from solutions 1 and 2. The ROB MEX orbits result in a global gain of precision of 33 m and of 8 m on the mean value and the standard deviation of the post-fit residuals, respectively (values obtained by adding the gain in precision for the right ascension and the declination). This improvement is in accordance with the improvement of the ROB MEX orbit assessed from the overlap differences that we have obtained with respect to the overlap differences of the ESOC MEX orbits, and provides an external validation of the ROB MEX orbits.

We have also assessed the impact of using the ROB MEX orbit to derive the Phobos positions relative to Mars, by comparing directly the positions from solutions 1 and 2. Fig. 7 displays the difference of the Phobos positions

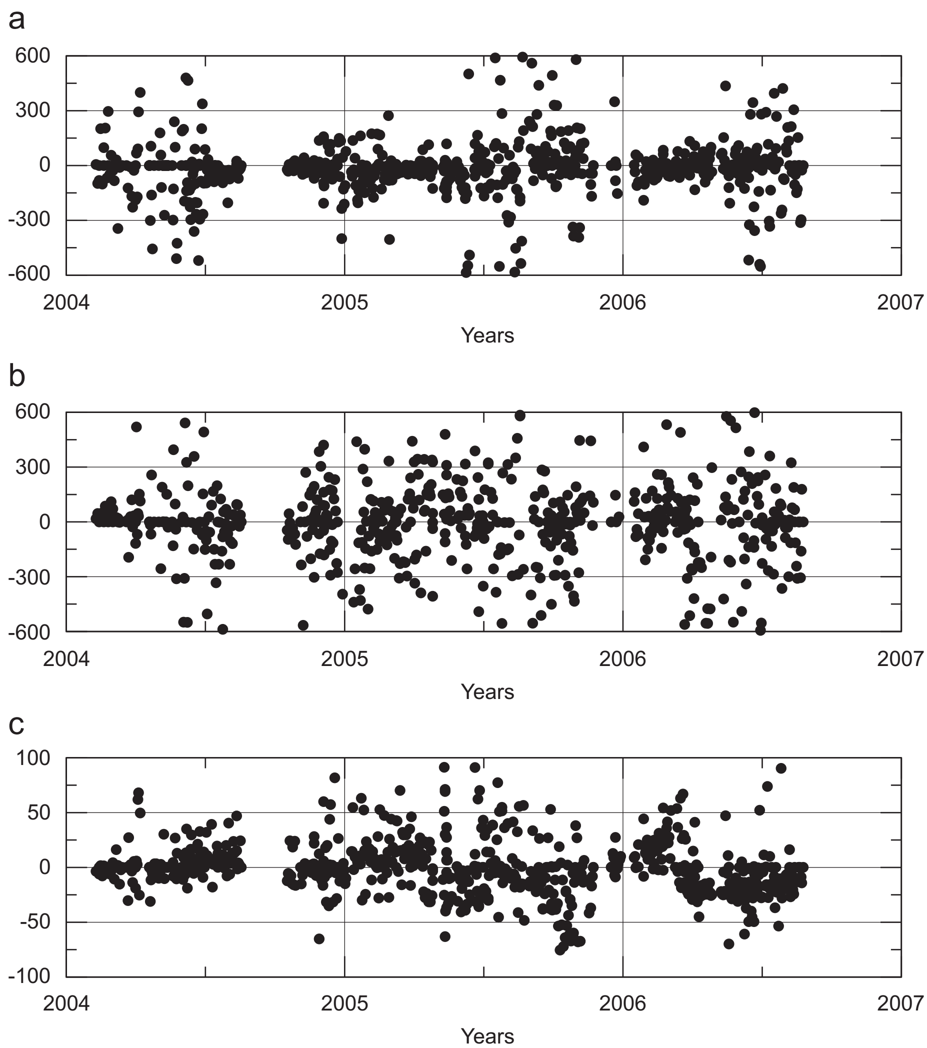

Fig. 4. Corrections to the residual acceleration at each WoL event expressed in percentage of the initial value for (a) the X-axis, (b) the Y-axis, and (c) the Z-axis components in reference frame tied to the spacecraft. The WoL event corresponds to the desaturation of the inertial wheels, which is needed to control the spacecraft attitude. These events daily occur in average.

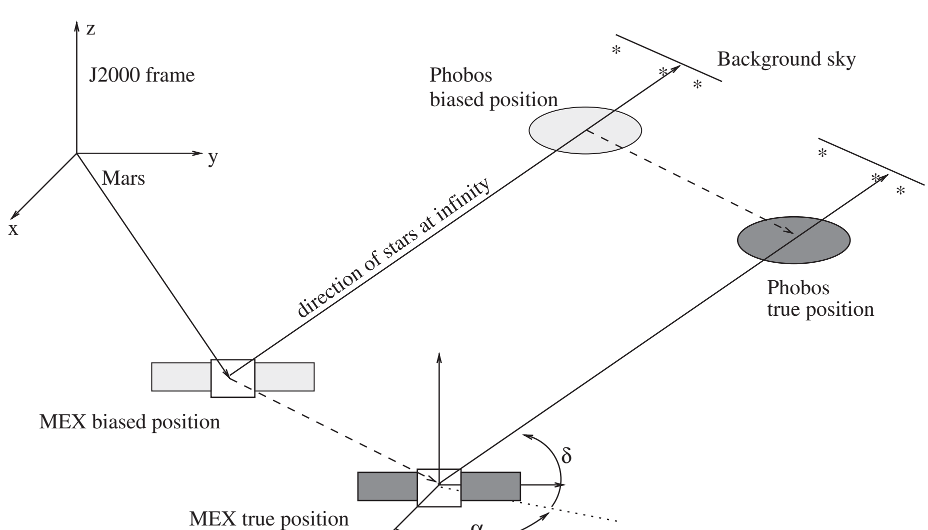

Fig. 5. Effect of the errors on MEX position to the Phobos position.

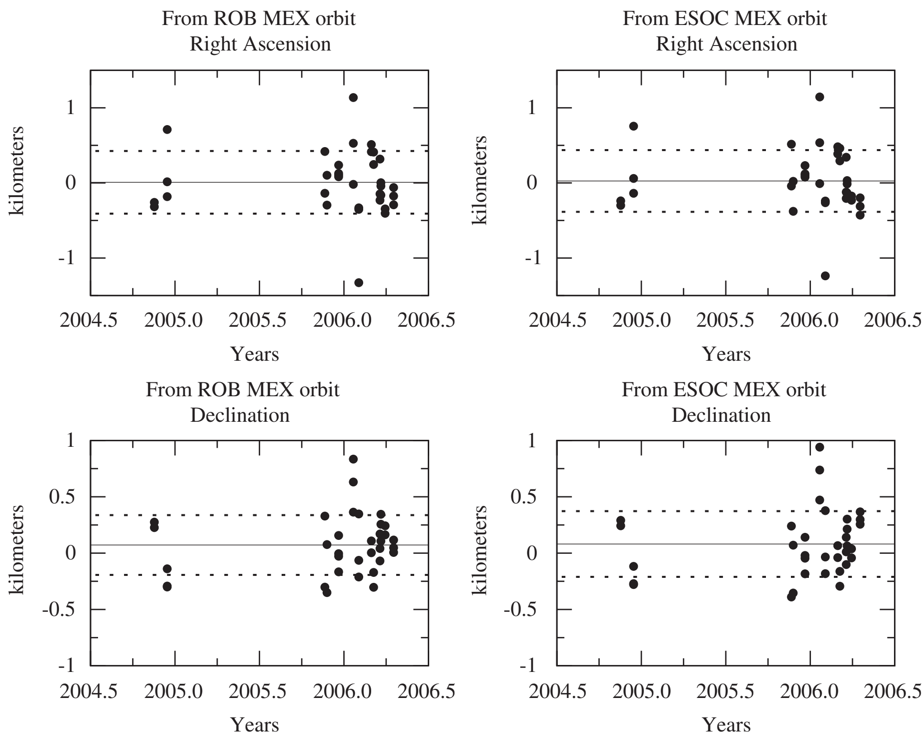

Fig. 6. Post-fit residuals of the Phobos orbital positions using ROB MEX orbit (solution 1) versus ESOC MEX orbit (solution 2) for the 34 selected SRC observations (see text).

Table 1
Mean ($\langle v \rangle$) and standard deviation (σ) on right ascension and declination of Phobos

Observations	$\langle v_\alpha \rangle$ (km)	σ_α (km)	$\langle v_\delta \rangle$ (km)	σ_δ (km)	N
MEX (ESOC)	0.035	0.412	0.078	0.278	34
MEX (ROB)	0.008	0.417	0.072	0.265	34

The angles have been multiplied by the distance between the point of observation and Phobos to provide values in kilometers. N denotes the number of observations (from Willner et al., 2007).

between both solutions over the 1982–2022 period. After the epoch of SRC observations, no more Phobos' observations have been introduced into both solutions, and the increase of the difference (up to 350 m over about 15 years) traduces a drift in the Phobos' positions from both solutions. This is not significant with respect to Mars' geophysical parameter, which can be extracted from the precise modeling of Phobos' motion such as Mars' tidal dissipation factor Q. However, our ROB MEX orbits should allow computing more precise Martian moon ephemerides for the preparation of future spacecraft missions.

5. Improvement of the determination of the mass of the Martian moons

The gravitational attraction of the Martian moons causes velocity variations of a Martian spacecraft, which can be detected from tracking data, especially when it is flying by at close distances. Various solutions of the mass (or the *GM* value) of the two moons were obtained from two independent Doppler data sets provided by the Viking 1 and 2 orbiters (Christensen et al., 1977; Tolson et al., 1977; Williams et al., 1988; Yuan et al., 2001) and by the Phobos 2 spacecraft for the Phobos mass (Berthias, 1990; Kolyuka et al., 1990). The Viking 1 orbiter performed a few flybys (or close encounter events) of Phobos at a distance of less than 350 km and the Viking 2 performed one single flyby of Deimos at a distance of 30 km. While the Viking flybys lasted a few minutes each, the Phobos 2 spacecraft was continuously flying at a distance of less than 500 km to Phobos during one week, providing a continuous flyby. Thus, the Phobos mass solution from the Phobos 2 data provided a solution with a relative error of less than 1% versus 15% for the Viking 1 solutions. Nevertheless, the solutions vary between the studies by up to 30%, suggesting that each solution could be corrupted by systematic errors. Indeed, the flyby solutions rely on the correct determination of both spacecraft and moon positions at the time of the encounter, thus any bias on these positions generate a bias on the moon mass determination. The Phobos 2 solutions were difficult to evaluate because of limited description of the data and of their processing.

On the other hand, the Martian moon gravitational attraction is regularly sensed by the spacecraft along its orbit around Mars, even if the distance to the moons is larger than during the flyby events. The associated force

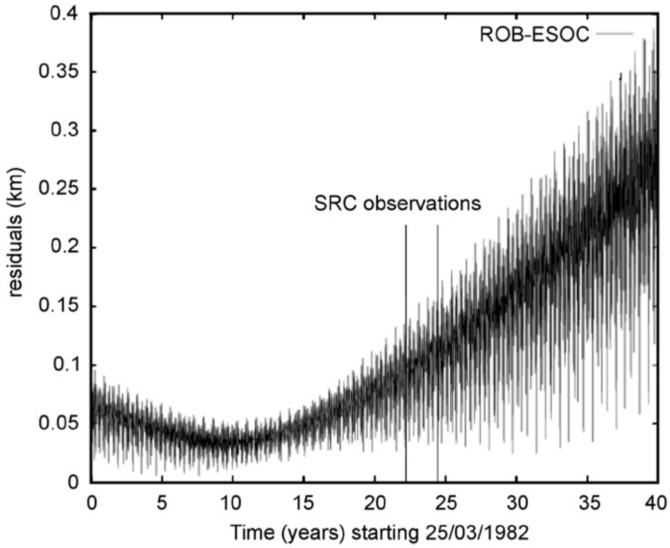

Fig. 7. Difference between the Phobos positions computed by using ROB (solution 1) and ESOC (solution 2) MEX orbits for the 34 SRC observations (see text).

causes a small secular drift of the orbital elements of the spacecraft from which the *GM* of the moons could be estimated. This method has been first employed by Smith et al. (1995) with tracking data of the former Mariner 9 and Viking 1 and 2 spacecraft.[1] The secular solution that they have found has a formal error comparable to the flyby ones, thus showing that estimates of the Martian moon *GM* can also be obtained from the monitoring of the small secular drift of the spacecraft orbit. However, their solutions still differ from the flyby solutions by up to 40% (see Table 4 in Smith et al., 1995). One possible explanation is that the resolution of Mars' gravity field used in that study was too weak to properly separate the effect of the Martian moon gravitational attractions from the effect of the shortest wavelengths of Mars' gravity field on the orbiter motion.

More recently Konopliv et al. (2006) have re-estimated the *GM* of both Martian moons from the monitoring of the MGS and ODY spacecrafts (secular solution) and from the Viking flybys. Their secular solutions show better uncertainties than the solutions from Smith et al. (1995) by a factor of about 3, mainly because of the improvement of Mars' orientation and gravity model. Given the uncertainties, their solutions are in agreement with most of the previous solutions from flybys (see Table 8 in Konopliv et al., 2006). Their Viking solution for the *GM* of Phobos is remarkably close to the Phobos 2 solution found by Berthias (1990) with a comparable uncertainty, providing a similar solution obtained from two independent Doppler data sets so far.

Since the MEX orbit has a semi-major axis about 3 times larger than the semi-major axis of MGS or ODY, the secular drift of its orbit, due to both Martian moon masses, is larger than the secular drift of MGS/ODY orbits. We have re-estimated the Martian moon *GM* by stacking together the normal equations resulting from the least squares fit performed on each MEX data-arc. The dynamical parameters for each data-arc (or local parameters) have been fitted together with the two *GM* (global parameters). No a priori constraint has been used for the *GM* parameters. We obtained a value of $0.711 \pm 0.002 \times 10^6\,\mathrm{m}^3/\mathrm{s}^2$ and $0.10 \pm 0.06 \times 10^6\,\mathrm{m}^3/\mathrm{s}^2$ for Phobos and Deimos, respectively. The formal uncertainties have been multiplied by a factor of 10 as done in Konopliv et al. (2006) for the MGS/ODY solutions. As expected, our solutions are in agreement with the secular solutions found by Konopliv et al. (2006), providing a smaller error for the *GM* of Phobos (Fig. 8). Our Phobos *GM* solution is, however, slightly different from the value of $0.716 \pm 0.0005 \times 10^6\,\mathrm{m}^3/\mathrm{s}^2$ found by Konopliv et al. (2006) from the Viking flyby data. Their formal error is, however, comparable to our formal error since these authors have scaled up the formal uncertainty of their Viking solution by a factor of only 2. In contrast to these authors, we did not adjust the Martian moon ephemerides together with the *GM* parameter. However, we have used up-to-date ephemerides, and their residual errors may not significantly contribute to the errors on the estimated *GM*. The small discrepancy between the MEX and Viking solution may also come from the two different approaches that have been used: secular versus flyby approach. In the latter approach the signal is largely dominated by the effect of the *GM* of the moon while in the former approach the signal is smaller and a part of it can be absorbed in the fit of the data-arc local parameters such as the initial state vector. The formal uncertainty on the *GM* of Deimos is

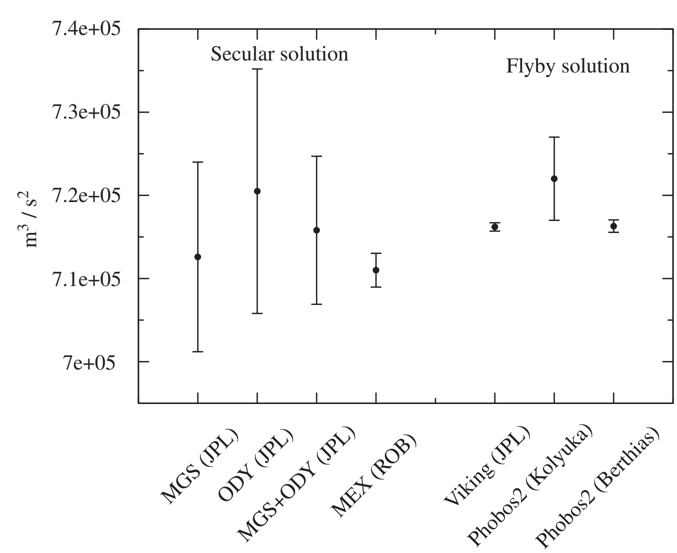

Fig. 8. Fit of Phobos' *GM*. The JPL solutions refer to Konopliv et al. (2006), the Phobos 2 solutions to Kolyuka et al. (1990) and Berthias (1990), and the ROB solution to this paper. The MGS, ODY, and MEX formal errors have been scaled up by a factor of 10 and the JPL Viking error by a factor of 2.

[1]In the rest of the paper, we choose to employ the terminology of 'secular solution' to refer to the solution based on this approach.

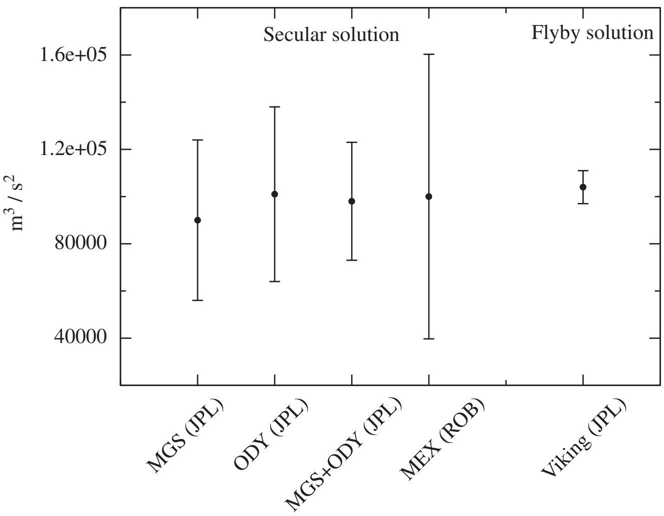

Fig. 9. Fit of Deimos' *GM*. The JPL solutions refer to Konopliv et al. (2006), and the ROB solution to this paper. The MGS, ODY and MEX formal errors have been scaled up by a factor of 10 and the JPL Viking error by a factor of 2.

larger than the uncertainty from the secular solution obtained by Konopliv et al. (2006) (Fig. 9). This is certainly due to the weaker signal of the mass of the more distant Deimos, which could not be well resolved from the stacking of only one Martian year of MEX tracking data, as performed in this study. A significant improvement is, however, expected when the stacking of more data-arcs will be achieved with the extended phase of the mission (at the end of 2009). In spite of its large uncertainty, our secular solution is in accordance with the solution from the single Viking 2 flyby at a distance of 30 km (Konopliv et al., 2006).

The estimates of the *GM* of the Martian moons from our MEX orbits are especially limited by the resolution of the acceleration at each WoL event. Indeed, when increasing the value of the a priori constraints on these local parameters, the values of the secular solution for the two *GM* slightly decreases. However, the error bars for these values still overlap with the error bars shown in Figs. 8 and 9. This means that part of the information coming from the *GM* is also absorbed in the fit of the WoL residual accelerations. This is particularly the case for the *GM* of Deimos since its larger distance from MEX provides lower perturbations on the MEX motion than the *GM* of Phobos does. Nevertheless, this limitation may be overcome by stacking more data-arcs.

Up to now, tracking data of MEX have been acquired at the closest MEX-Phobos distance of 465 km that occurred on March 23rd, 2006. A preliminary study by Andert et al. (2006) has used the MEX Doppler data at this closest encounter event only, and found a value of $0.77 \pm 0.04 \times 10^6\,m^3/s^2$ (formal error equal to the formal uncertainty). However, this solution was difficult to obtain from the tracking data because the expected signal of the Phobos mass at a distance of 465 km is just above the noise of the tracking data. A refinement of this estimation is being performed, and a new solution tends toward a value of $0.72 \times 10^6\,m^3/s^2$ (T. Andert, pers. comm., 2007), which is more in agreement with the secular solution found in this paper. This gives us confidence in the ability to significantly improve the determination of the Phobos mass from a close MEX flyby at a distance below the closest distance of 465 km performed so far.

6. Conclusions and perspectives

The tracking data of the Mars Express (MEX) spacecraft, performed by the Mars Express Radio-Science (MaRS) experiment, allows computing a MEX orbit with an average accuracy of 20–25 m. This accuracy is limited by the non-uniform distribution of the tracking data. The masses of the Martian moons have been re-estimated, and the uncertainty on the mass of Phobos is better than the uncertainty of the solution from the Mars Global Surveyor (MGS) and Mars Odyssey (ODY) spacecraft due to the higher semi-major axis of the MEX orbit. Better estimates are expected thanks to the additional tracking data of the next extended phase of the mission (up to 2009). A possibility to improve the accuracy of the MEX orbits would be to perform MEX orbit determination with non-successive data-arcs with variable duration in order to avoid periods when gaps in the tracking coverage are too numerous and/or too long. Such possibility will be investigated in order to improve the determination of the seasonal changes of the first zonal harmonics of Mars' gravity field from a combination of both MGS, ODY and MEX tracking data sets (Rosenblatt et al., 2005). In addition to the refinement of the Phobos mass determination, future MEX-Phobos close flybys would also provide the opportunity to determine the second-order coefficients of the gravity field of Phobos. Lainey et al. (2007) tried to estimate the C_{20} and C_{22} coefficients from the fit of their ephemerides, but they could not provide reliable results. At a MEX-Phobos distance of about 100 km, these coefficients are expected to produce a perturbation of the MEX motion, which is within 1% of the perturbation associated with the *GM*. As the mass is already known at a precision of less than 0.1%, it would be possible to improve the determination of these second-order coefficients from tracking data of future MEX-Phobos close flybys (at a distance of less than 100–150 km). Such improvement would allow better constraining the repartition of the distribution of mass within Phobos.

This paper has also shown the interest to merge both space geodesy and the orbital dynamics approaches to enhance the information contained in both astrometrical observations and spacecraft tracking data. Such strategy could be applied to increase the scientific return of the future missions like the Europa orbiter of the Laplace mission proposed for the ESA cosmic vision.

Our MEX ROB orbits are available as SPICE kernels at the NAIF web site (http://naif.jpl.nasa.gov/naif).

Acknowledgments

The authors are greatly indebted to K. Willner and J. Oberst for providing the latest Martian moon observations, including the newest reductions of the SRC instrument data. The authors also thank T. Morley, F. Budnik and their colleagues of the ESOC Flight Dynamics team for providing all the needed information about the MEX spacecraft and for fruitful discussion about the ESOC MEX orbit. The authors thank R. Simpson for providing as much MEX DSN-tracking data as possible. The reviews by A. Konopliv and an anonymous reviewer have been helpful to clarify some points in the paper. The Belgian team, and in particular P. Rosenblatt and S. Le Maistre are financially supported by the Belgian PRODEX program managed by the European Space Agency in collaboration with the Belgian Federal Science Policy Office. M. Pätzold acknowledges support from Bundesministerium für Wirtschaft (BMWi) via DLR under Grant 50QM0701. B. Häusler is funded by the German Bundesministerium für Wirtschaft und Technologie under DLR Grant 50 QM 04 01.

References

Andert, T.P., Pätzold, M., Rosenblatt, P., Lainey, V., Marty, J.C., Le Maistre, S., Häusler, B., 2006. Mass estimate of the moon Phobos from the Mars Express Radio Science Experiment MaRS. In: 38th Annual DPS Meeting, October 8–13, Pasadena, CA.

Berthias, J., 1990. Analysis of the Phobos 2 radiometric data set. JPL IOM 314.6-1129. Jet Propulsion Laboratory, California Institute of Technology, Pasadena, CA.

Bruinsma, S., Lemoine, F.G., 2002. A preliminary semiempirical thermosphere model of Mars: DTM-Mars. J. Geophys. Res. 107 (E10), 5085, doi:10.1029/2001JE001508.

Christensen, E.J., Born, G.H., Hildebrand, C.E., Williams, B.G., 1977. The mass of Phobos from Viking flybys. Geophys. Res. Lett. 4, 555.

Duron, J., Marty, J.C., Balmino, G., Rosenblatt., P., Le Maistre, S., Dehant, V., 2006. Time variations of Mars gravity field from Mars Global Surveyor and Odyssey data. AGU Fall Meeting, San Francisco, CA.

Folkner, W., 2007. Current developments in the JPL planetary ephemerides. In: First European Workshop on Solar System Dynamics and Ephemerides, ESOC, Darmstadt, Germany.

Highsmith, D.E., Konopliv, A.S., Han, D., Jah, M.K., Craig, D.E., 2004. Mars atmospheric variability above 250 km altitude. In: 18th International Symposium on Space Flight Dynamics, October 11–15, 2004, Munich, Germany.

Kolyuka, Y.F., Efimov, A.E., Kudryavtsev, S.M., Margorin, O.K., Tarasov, V.P., Tikonov, V.F., 1990. Refinement of the gravitational constant of Phobos from Phobos 2 tracking data. Sov. Astron. Lett. 16 (March–April), 168–170.

Konopliv, A.S., Yoder, C.F., Standish, E.M., Yuan, D.N., Sjogren, W.L., 2006. A global solution for the Mars static and seasonal gravity, Mars orientation, Phobos and Deimos masses, and Mars ephemeris. Icarus 182, 23–50.

Lainey, V., Dehant, V., Pätzold, M., 2007. First numerical ephemerides of the Martian moons. Astron. Astrophys. 465, 1075.

Lemoine, F.G., 1992. Mars: the dynamics of orbiting satellites and gravity model development. Ph.D. Thesis, University of Colorado, Boulder, CO.

Oberst, J., Matz, K.D., Roatsch, T., Giese, B., Hoffmann, H., Duxbury, T., Neukum, G., 2006. Astrometric observations of Phobos and Deimos with the SRC on Mars Express. Astron. Astrophys. 447, 1145.

Pulido-Cobo, J.A., Schoenmaekers, J., 2004. Combined control of the operational Mars Express orbit and the spacecraft angular momentum. In: 18th International Symposium on Space Flight Dynamics, October 11–15, 2004, Munich, Germany.

Rosenblatt, P., Marty, J.C., Perosanz, F., Barriot, J.P., van Hoolst, T., Dehant, V., 2004. Numerical simulations of a Mars geodesy network experiment: effect of orbiter angular momentum desaturation on Mars' rotation estimation. Planet. Space Sci. 52, 965.

Rosenblatt, P., Duron, J., Marty, J.C., Dehant, V., Pätzold, M., Häusler, B., Le Maistre, S., Karatekin, Ö., van Hoolst, T., Balmino, G., 2005. A new solution of Mars' time variable gravity field from a joint inversion of MEX and MGS radio-tracking data. AGU Fall Meeting, San Francisco, CA, doi:10.1029/2001JE001508.

Smith, D.E., Lemoine, F.G., Zuber, M.T., 1995. Simultaneous estimation of the masses of Mars, Phobos, and Deimos using spacecraft distant encounters. Geophys. Res. Lett. 22 (16), 2171–2174.

Stewart, A.I.F., 1987. Revised time dependent model of the Martian atmosphere for use in orbit lifetime and sustenance studies. Technical Report JPL PO NQ-802429, University of Colorado, Boulder, Co.

Tolson, R.H., Blackshear, W.T., Mason, M.L., 1977. The mass of Phobos. Geophys. Res. Lett. 4, 551.

Williams, B.G., Duxbury, T.C., Hildebrand, C.E., 1988. Improved determination of Phobos and Deimos masses from Viking flybys. Lunar and Planetary Science Conference, vol. XIX, p. 1274.

Willner, K., Oberst, J., Matz, K.-D., Wählisch, M., Giese, B., Roatsch, T., Hoffmann, H., Neukum, G., 2007. Observations of Phobos' orbit and rotation using images of SRC on Mars Express. In: European Mars Science and Exploration Conference: Mars Express and Exomars, ESTEC, Noordwijk, The Netherlands.

Yuan, D.N., Sjogren, W.L., Konopliv, A.S., Kucinskas, A.B., 2001. Gravity field of Mars: a 75th degree and order model. J. Geophys. Res. 106, 23377.